

## OZONE TRANSPORT ANALYSIS USING BACK-TRAJECTORIES AND CAMx PROBING TOOLS

Greg Yarwood\*, Susan Kemball-Cook, Bonyoung Koo and Jeremiah Johnson  
ENVIRON International Corporation, Novato, CA, USA

Jim Price and Mark Estes  
Texas Commission on Environmental Quality, Austin, TX, USA

### 1. INTRODUCTION

Lowering the 8-hour ozone standard increases the importance of background ozone and transport in contributing to ozone nonattainment. Accurate simulation of ozone transport in photochemical grid models will be critical for the development of effective ozone control strategies. This study evaluated modeled ozone transport in the Comprehensive Air quality Model with extensions (CAMx; ENVIRON, 2010) photochemical model for several Texas ozone episodes, and used CAMx probing tools to assess transport contributions and their response to potential emission changes.

The modeled representation of transport pathways from ozone source regions into Texas was investigated by comparing Hybrid Single Particle Lagrangian Integrated Trajectory Model (HYSPLIT; Draxler and Hess, 1997) back trajectories based on Eta Data Assimilation System (EDAS) meteorology with back trajectories based on the MM5 meteorological data supplied as input to CAMx. The CAMx Anthropogenic Precursor Culpability Assessment (APCA) tool and the CAMx Higher Order Decoupled Direct Method (HDDM; Dunker et al., 2002) tool were used to provide complementary information on upwind source contributions to Texas ozone. HDDM was also used to evaluate the sensitivity of Texas ozone to potential changes in emissions in upwind source regions.

### 2. MODEL CONFIGURATION

CAMx was applied for three Texas high ozone episodes in 2005-6 using an updated vertical transport algorithm and the Zhang dry deposition algorithm (Zhang et al. 2003; Zhang et al. 2008), which are newly implemented in CAMx version 5.21. The Zhang algorithm is a leaf area index (LAI)-based, state-of-the-science scheme which is

used in Environment Canada's A Unified Regional Air-quality Modeling System (AURAMS) air quality model and has an updated representation of non-stomatal deposition pathways. The Zhang algorithm has been tested extensively through its use in daily air quality forecasting and has been shown to reproduce observed fluxes of ozone and SO<sub>2</sub> with reasonable accuracy. During its implementation in CAMx, the capabilities of the Zhang scheme were extended by adding the option to use episode-specific satellite LAI data.

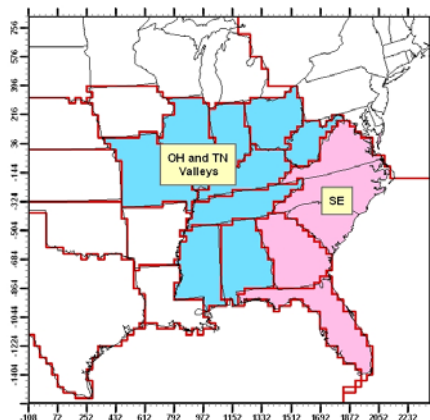


Figure 1. Source regions within the 36 km grid. APCA source regions are indicated by red borders and HDDM source regions are shaded. The Ohio-Tennessee Valley region (OH-TN) is shaded blue and the Southeastern U.S. (SE) region is shaded pink.

Periods of the 2005-6 Texas high ozone episodes favorable for the transport of ozone and precursors into Texas were identified from HYSPLIT back trajectories based on EDAS meteorological fields and analyses of ambient ozone data from rural upwind monitoring sites. Potential source regions were also identified as shown in Figure 1. As an example of the analysis carried out for all of the 2005-6 transport episodes, we focus here on one of these episodes, June 13-15, 2006.

\*Corresponding author: Greg Yarwood, ENVIRON, International Corporation, 773 San Marin Dr, Novato, CA, 94998; e-mail: [gyarwood@environcorp.com](mailto:gyarwood@environcorp.com).

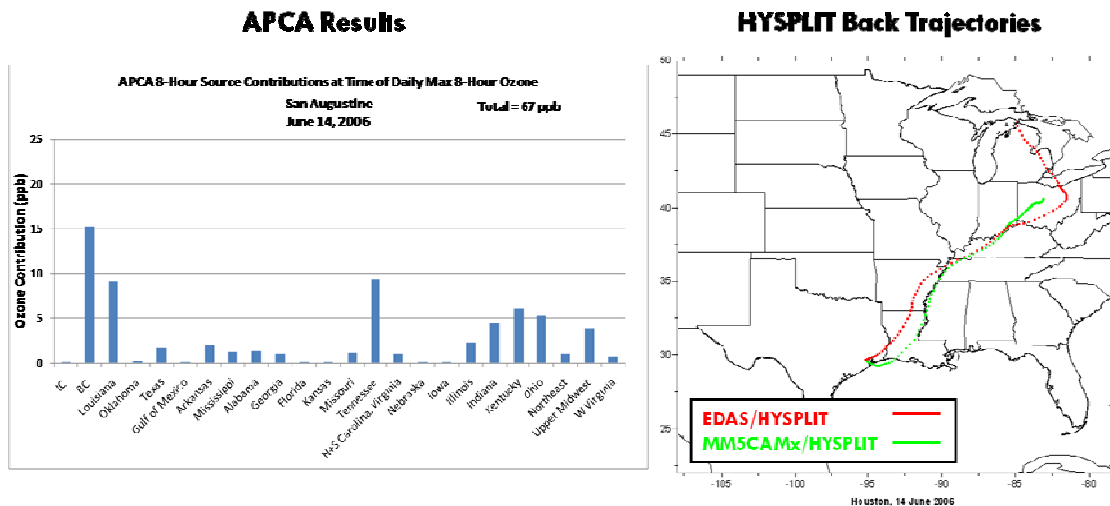


Figure 2. Left panel: APCA source apportionment for the San Augustine, Texas monitor on June 14, 2006 at the time of the daily max 8-hour ozone value. Right panel: HYSPLIT model 96-hour back trajectories ending at 250 meters using EDAS (red) and MM5CAMx (green) meteorological inputs to HYSPLIT.

CAMx ozone performance during the transport period was evaluated at rural monitors within Texas, in adjacent states, and in potential source regions further upwind. CAMx simulated ozone at rural sites with good accuracy during the transport period.

The modeling was performed on a 36 km grid that covered the eastern U.S. (Figure 1) and a nested 12 km grid focused on Texas and surrounding states; the 36 km grid was divided into source regions for the APCA and HDDM analyses as shown in Figure 1.

For the APCA source apportionment, most states were treated as individual source regions. For the HDDM analysis, individual states in the Ohio and Tennessee Valleys and the Southeastern U.S. were aggregated to form two larger source regions. The emission inventory was divided into three emissions source categories: elevated anthropogenic emissions, biogenic emissions, and all other emissions. The main component of the elevated anthropogenic NOx emission inventory is electric generating unit emissions.

### 3. MODEL TRANSPORT ASSESSMENT

The model transport assessment evaluated the performance of CAMx in characterizing transport pathways that can bring ozone from the source regions into Texas. Several CAMx tools were used together to analyze different aspects of this multi-day period when ozone transport from areas outside of Texas into East Texas likely occurred.

A new tool that generates HYSPLIT back trajectories based on the MM5CAMx horizontal wind fields input to CAMx and the CAMx vertical velocity algorithm was used to assess the accuracy of the model winds during the transport episode. By comparing HYSPLIT back trajectories made using EDAS inputs to otherwise identical HYSPLIT back trajectories made with MM5CAMx inputs, potential problems with ozone transport due to errors in modeled winds may be diagnosed. Back trajectories computed with data from EDAS and MM5CAMx are compared in Figure 2 for June 14, 2006 and show good agreement.

The APCA tool was used to determine which upwind ozone source regions contributed to high ozone at Texas monitors during the episode. Then, the HDDM tool was used to examine how ozone at receptors in Texas would be affected by reductions in emissions in the ozone source regions and by changes in the biogenic emission inventory.

#### 3.1 APCA Source Apportionment Analysis

The APCA tool was used to quantify contributions by source region and source category to ozone at a given receptor and time. As an example, the APCA source apportionment for the San Augustine, TX monitor (abbreviated SAGA in Figure 3) for the June 14 high ozone day is shown in Figure 2. The largest contributors to peak ozone at San Augustine are the boundary

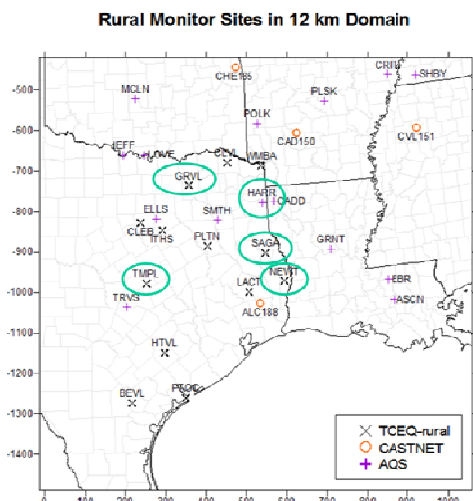


Figure 3. Rural ozone monitors within the 12 km grid. Monitors circled in green were used in the APCA/HDDM analysis.

conditions, Louisiana, Tennessee, Kentucky, Ohio, and other states in the Ohio and Tennessee Valleys. June 14 was a day when the source regions outside Texas had a much larger effect on ozone at San Augustine than sources within Texas. The importance of the Ohio and Tennessee Valleys in the source apportionment is consistent with the HYSPLIT back trajectories, which show air from this source region arriving at the monitor on June 14. The similarity of the HYSPLIT back trajectories made with EDAS and the MM5CAMx winds corroborate the modeled winds for the days leading up to June 14.

### 3.2 HDDM Emissions Sensitivity Analysis

APCA analyses similar to that shown in the previous section for June 14 established the importance of the transported contribution to ozone measured at other Texas rural monitors during the June 13-15, 2006 ozone episode. The HDDM tool was then used to determine the sensitivity of ozone at the Texas rural monitors during this period to changes in emissions in the Ohio and Tennessee Valley source region (abbreviated OH-TN below) as well as in the rest of the modeling domain.

We evaluated the sensitivity of the daily maximum 8-hour ozone throughout the domain to changes in elevated anthropogenic NOx emissions in the OH-TN source region. The following first and second order sensitivities,  $S^1$  and  $S^2$ , of surface layer ozone to elevated anthropogenic NOx emissions (eaNOx) in the source regions were calculated:

$$S^1_{OH-TN} \sim \frac{\partial O_3}{\partial(eaNOx_{OH-TN})}, \quad S^1_{SE} \sim \frac{\partial O_3}{\partial(eaNOx_{SE})}, \quad (1)$$

$$S^2_{OH-TN} \sim \frac{\partial^2 O_3}{\partial(eaNOx_{OH-TN})^2}, \quad S^2_{SE} \sim \frac{\partial^2 O_3}{\partial(eaNOx_{SE})^2}, \quad (2)$$

where OH-TN indicates the source region shown in blue in Figure 1. The sensitivities were averaged across the June 13-15 episode for all grid cells within the 36 km domain at all times when the 8-hour ozone in each grid cell was greater than 60 ppb. This excluded periods of low ozone from the analysis. By examining spatial maps of the sensitivity coefficients, we can determine how sensitive ozone throughout the 36 km domain is to emissions changes in the source regions.

Figure 4 shows the June 13-15 episode average  $S^1_{OH-TN}$  and  $S^2_{OH-TN}$ .  $S^1_{OH-TN}$  is generally positive. A positive value of  $S^1_{OH-TN}$  means that ozone increases (decreases) if eaNOx emissions in the OH-TN Valley source region increase (decrease). The sensitivity of ozone to the eaNOx emissions is largest in the source region.  $S^1_{OH-TN}$  is negative in the vicinity of large NOx sources, indicating that a decrease in eaNOx emissions would increase ozone locally. This occurs when NOx emissions from a large source suppress ozone in its vicinity. When NOx emissions are reduced, titration of ozone is lessened so that the NOx reduction increases ozone (NOx disbenefit).

Figure 4 indicates that there is an east-west gradient in  $S^1_{OH-TN}$  across Texas, and that  $S^1_{OH-TN}$  ranges from approximately 1-4 ppb on average in East Texas over the June 13-15 episode. This indicates that ozone in East Texas is sensitive to changes in eaNOx emissions in the OH-TN source region.

The second order term  $S^2_{OH-TN}$  has mostly negative values within the 36 km domain that are smaller in absolute magnitude than the  $S^1_{OH-TN}$  sensitivity.  $S^2_{OH-TN}$  has its largest absolute value in the vicinity of large, coal-fired power plants along the Ohio River. This indicates that nonlinearity is greatest in the source region, while, outside the source region, the linear first order term dominates. Values of  $S^2_{OH-TN}$  in East Texas are small compared to the first order sensitivity, but are not zero. We can conclude from the sensitivities shown in Figure 4 that Texas ozone is sensitive to emissions

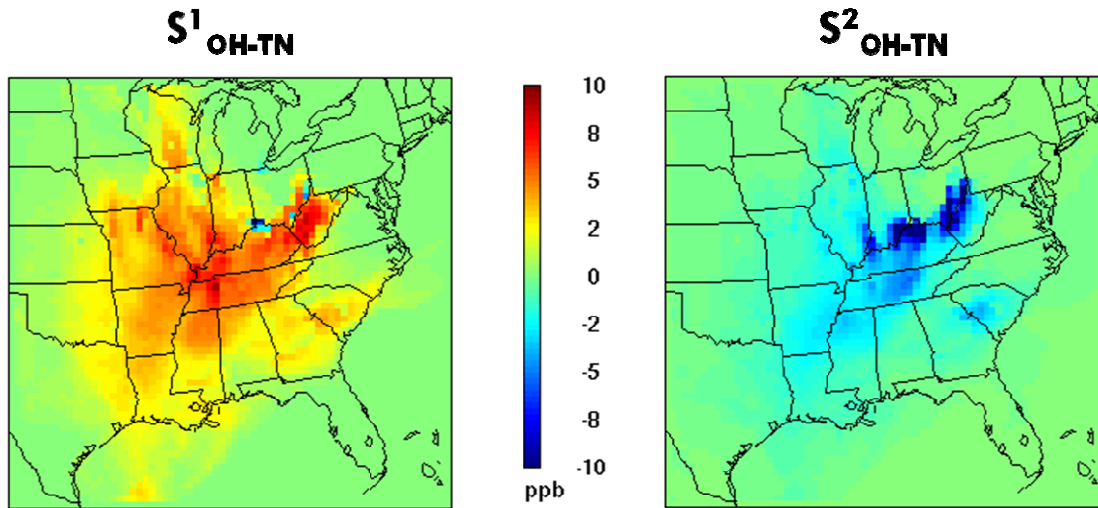


Figure 4. June 13-15, 2006 average  $S^1_{OH-TN}$  and  $S^2_{OH-TN}$ . For each grid cell, times when ozone values were less than 60 ppb were excluded from the average.

changes in the OH-TN source region during this episode, and that the relationship between emissions reductions in the source region and ozone at East Texas receptors has some inherent non-linearity. The nonlinearity indicated by the non-zero  $S^2$  term shows that estimating the effects of potential emissions reductions by scaling the OH-TN APCA ozone contributions would result in a bias toward overestimating benefits. HDDM results can quantify the magnitude of ozone changes at specific receptors in East Texas in response to reductions in eaNOx emissions in the OH-TN source region.

We use the HDDM coefficients to calculate the ozone change at a given receptor that would result from an emissions change about an unperturbed state (Hakami et al., 2003). We follow the notation of Hakami and denote ozone concentration by  $C$ . We examine the effect of an emissions perturbation  $\Delta\epsilon$  by expanding the ozone concentration in a Taylor series about an unperturbed state,  $C(0)$ . The sensitivities  $S^{(i)}$  are given by  $\partial C/\partial\epsilon$  in this notation. The Taylor expansion is:

$$C(+\Delta\epsilon) = C(0) + \Delta\epsilon S^{(1)}(0) + \frac{\Delta\epsilon^2}{2} S^{(2)}(0) + \dots + \frac{\Delta\epsilon^n}{n!} S^{(n)}(0) + R_{n+1} \quad (3)$$

where we neglect the higher order terms  $R_{n+1}$ . We examine the change in ozone that would result from an eaNOx emissions reduction within the source region. This corresponds to varying  $\Delta\epsilon$

and calculating the corresponding change in ozone at the receptor,  $C(\Delta\epsilon) - C(0)$ . For example,  $\Delta\epsilon = -0.20$  for a 20% emissions reduction in the source region, and  $C(0)$  = daily max 8-hour ozone at the monitor in the unperturbed case. We can then plot the emissions change  $\Delta\epsilon$  versus the change in ozone  $C(\Delta\epsilon) - C(0)$  at each monitor. Figure 5 shows the change in daily maximum 8-hour ozone at several rural Texas receptors that would result from reducing eaNOx in the OT source region. Only results for June 14 are shown in Figure 5, but the results for the rest of the episode are similar. Figure 5 indicates that all of the Texas rural monitors would see a reduction in daily max 8-hour ozone during this episode if eaNOx emissions were decreased in the OH-TN source region. Of all of the rural Texas monitors considered here, the Newton (NEWT in Figure 3) and San Augustine monitors show the largest ozone decreases in response to OH-TN eaNOx emissions reductions.

The first and second order HDDM sensitivities can also be used to estimate the effect on ozone of removing (zeroing out) one or more emissions sources. For two emissions sources  $j$  and  $k$ , the zero out contribution (ZOC) is calculated (Cohan et al., 2005),

$$ZOC(P_j + P_k) \approx \underbrace{(S_j^{(1)} - \frac{1}{2}S_{j,j}^{(2)})}_{ZOC_j} + \underbrace{(S_k^{(1)} - \frac{1}{2}S_{k,k}^{(2)})}_{ZOC_k} - \underbrace{S_{j,k}^{(2)}}_{cross\ term} \quad (4)$$

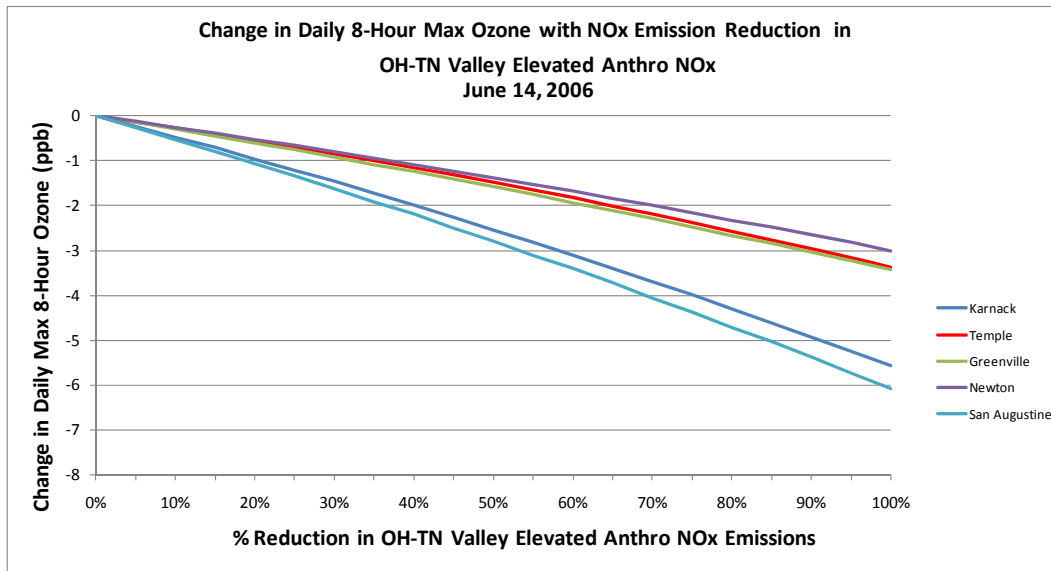


Figure 5. Change in daily max 8-hour ozone at rural Texas monitors with OH-TN eaNOx emissions reduction.

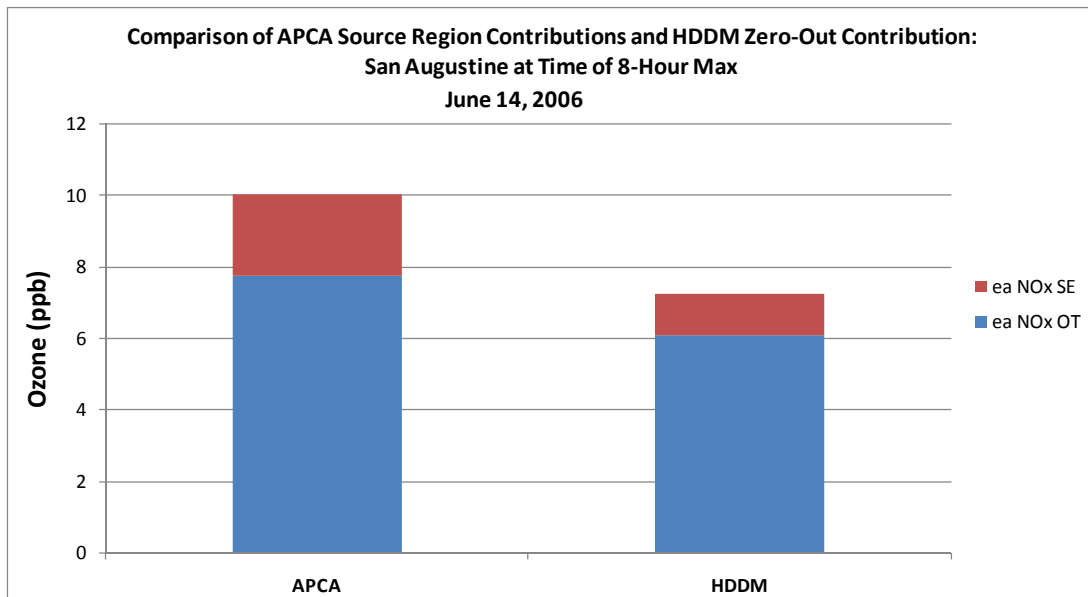


Figure 6. June 14, 2006 comparison of APCA and HDDM ZOC estimates for eaNOx.

For the OH-TN and SE source regions, the ZOC is given by

$$\text{ZOC}_{(\text{OT}+\text{SE})} \approx (\text{S}_{\text{OT}}^{(1)} - \frac{1}{2}\text{S}_{\text{OT,OT}}^{(2)}) + (\text{S}_{\text{SE}}^{(1)} - \frac{1}{2}\text{S}_{\text{SE,SE}}^{(2)}) - \text{S}_{\text{OT,SE}}^{(2)} \quad (5)$$

Below, we present only the components of the ZOC for OH-TN and SE eaNO<sub>x</sub> emissions, as the cross term  $\text{S}_{\text{OT,SE}}^{(2)}$  was negligible. A positive ZOC corresponds to an ozone decrease at a receptor upon removal of the source in question. The ZOC derived from the HDDM sensitivities may be compared with the APCA contributions totaled from states comprising the SE and OH-TN (OT) source regions used in the HDDM analysis.

Figure 6 compares the APCA ozone contributions from eaNO<sub>x</sub> and the ZOC from OH-TN and SE eaNO<sub>x</sub>. Both the APCA and HDDM probing tools ascribe a larger contribution to the OH-TN source region than to the SE source region. The APCA and HDDM tools are in agreement with one another on the relative importance of these two source regions in contributing to high ozone in Texas, and are consistent with the HYSPLIT back trajectories shown in the right panel of Figure 2, which pass over the OH-TN states but not the SE states. Because these three tools, independent of each other and having different formulations, give similar results, greater confidence may be placed in the source attribution than if only a single tool had been used.

#### 4. CONCLUSIONS

We have shown how a suite of tools can be applied to analyze CAMx ozone transport. These tools provide complementary information on the model winds that define the transport pathway from source regions to receptor regions, ozone source apportionment, and sensitivity of receptors to emissions changes in the source regions. Because their formulations are independent of one another, each of these tools can serve as a way to evaluate information provided by the other tools. For example, the APCA and HDDM tools can both provide estimates of source apportionment, and the HYSPLIT back trajectories can be used to assess whether that source apportionment is reasonable. Used in combination, these tools can provide a valuable resource for control strategy development.

#### 5. REFERENCES

- Cohan, D.S., A. Hakami, Y. Hu, and A.G. Russell, 2005: Nonlinear response of ozone to emissions: Source apportionment and sensitivity analysis. *Environ. Sci. Tech.*, **39**, 6739-6748.
- Draxler, R.R. and G.D. Hess, 1997: Description of the Hysplit\_4 modeling system. NOAA Tech. Memo ERL ARL-224, Dec, 24 pp.
- Dunker, A. M., G. Yarwood, J. P. Ortmann, and G. M. Wilson, 2002: The decoupled direct method for sensitivity analysis in a three-dimensional air quality model—Implementation, accuracy, and efficiency. *Environ. Sci. Tech.* **36**, 2965-2976.
- ENVIRON, 2010: Users Guide: Comprehensive Air quality Model with Extensions (CAMx), Version 5.20 (April, 2010). ENVIRON International Corporation, Novato, California. [Available online at [www.camx.com](http://www.camx.com).].
- Hakami, A., M. T. Odman, and A. G. Russell, 2003: High-order, direct sensitivity analysis of multidimensional air quality models. *Environ. Sci. Technol.*, **37**, 2442.
- Zhang, L., J. R. Brook, and R. Vet, 2003: A revised parameterization for gaseous dry deposition in air-quality models. *Atmos. Chem. Phys.*, **3**, 2067–2082.
- Zhang, X., S. Kondragunta, C. Schmidt, and F. Kogan, 2008: Near real time monitoring of biomass burning particulate emissions (PM<sub>2.5</sub>) across contiguous United States using multiple satellite instruments. *Atmos. Environ.* **42**, 6959-6972.